Static and Dynamic Posterior Cingulate Cortex Nodal Topology of Default Mode Network Predicts Attention Task Performance

Pan Lin[1,3,6*],Yong Yang[2] ,Jorge Jovicich[3,4], Nicola De Pisapia[3], Xiang Wang[5],Chun S. Zuo[6],James Jonathan Levitt[7,8]

[1] Key Laboratory of Biomedical Information Engineering of Education Ministry,Institute of Biomedical Engineering, Xi'an Jiaotong University, Xi'an 710049, China
[2]School of Information Technology, Jiangxi University of Finance and Economics, Nanchang, People's Republic of China
[3]Center for Mind/Brain Sciences, University of Trento, Italy
[4]Department of Cognitive and Education Sciences, University of Trento, Italy
[5]Medical Psychological Institute of Second Xiangya Hospital,Central South University,Chang sha, China
[6]Brain Imaging Center, McLean Hospital, Department of Psychiatry, Harvard Medical School, Belmont, MA, USA.
[7]Clinical Neuroscience Division, Laboratory of Neuroscience, Department of Psychiatry, VA, Boston Healthcare System, Brockton Division, and Harvard Medical School, Boston, MA 02301, USA;
[8]Psychiatry Neuroimaging Laboratory, Department of Psychiatry, Brigham & Women's Hospital, Harvard Medical School, Boston, MA 02215, USA.

[*]Corresponding author: Pan Lin
Corresponding address: Key Laboratory of Biomedical Information Engineering of Education Ministry, Institute of Biomedical Engineering, Xi'an Jiaotong University, Xi'an 710049, China.

Email:linpan@mail.xjtu.edu.cn

Tel: 86- 13299059976
Fax number: 86-29-82668664

Short Title: Static and Dynamic Posterior Cingulate Cortex Nodal Topology and Task Performance

Keywords: Default Mode Network (DMN), Functional Connectivity (FC), Task Performance, Posterior Cingulate Cortex (PCC), Degree

Abstract

Characterization of the default mode network (DMN) as a complex network of functionally interacting dynamic systems has received great interest for the study of DMN neural mechanisms. In particular, understanding the relationship of intrinsic resting-state DMN brain network with cognitive behaviors is an important issue in healthy cognition and mental disorders. However, it is still unclear how DMN functional connectivity links to cognitive behaviors during resting-state. In this study, we hypothesize that static and dynamic DMN nodal topology associated with upcoming cognitive task performance. We used graph theory analysis in order to understand better the relationship between the DMN functional connectivity and cognitive behavior during resting-state and task performance. Nodal degree of the DMN was calculated as a metric of network topology. We found that the static and dynamic posterior cingulate cortex (PCC) nodal degree within the DMN was associated with task performance (Reaction Time). Our results show that the core node PCC nodal degree within the DMN was significantly correlated with reaction time, which suggests that the PCC plays a key role in supporting cognitive function.

Introduction

The intrinsic resting-state networks (RSN) have recently attracted increasing attention in neuroscience research. One prominent RSN is the default-mode network (DMN), which revealed highly correlated intrinsic low-frequency ***blood oxygenation level-dependent (BOLD)*** signal (Greicius et al., 2003) or metabolic activity (Buckner et al., 2008;Raichle and Gusnard, 2002) during resting-state together with task-induced deactivation (Buckner et al., 2008;Lin et al., 2011). The DMN is a special brain system that comprises a set of interacting brain regions, including medial prefrontal cortex (MPFC), posterior cingulate cortex (PCC), lateral and medial temporal lobes (MTL), and posterior inferior parietal lobule (pIPL) (Buckner et al., 2008). There is accumulating evidence that indicates that sub-regions of the DMN perform specialized functions (Buckner et al., 2008). For example, within DMN sub-regions or sub-nodes, PCC plays key roles in monitoring one's own internal state and emotions, self-referential processing, problem solving and task-independent thoughts, memory consolidation, social cognition and autobiographical memory (Buckner et al., 2008;Leech and Sharp, 2013;van Veluw and Chance, 2014). ***The PCC play a central role within the default network and their functional connectivity is supported by structural connectivity studies (Greicius et al., 2009;Patel et al., 2013). In addition, the PCC node shows a high metabolic rate during the baseline state (Raichle et al., 2001). PCC function might be particularly important for understanding brain function and the impact of disease on brain function (Leech and Sharp, 2013(Philip et al., 2013)). Accumulating studies suggest the PCC region, itself, has greater communication with other brain systems which allows it to support ongoing task performance (Leech and Sharp, 2013). Furthermore, most studies have supported the idea that functional integrity of the PCC***

may be related to executive control processes (Kelly et al., 2008). The DMN sub-regions may play important roles in regulating resources competition during attention and in supporting higher-level executive function tasks (Andrews-Hanna et al., 2007). In short, the PCC plays a central role in regulating the balance between internally and externally driven information for supporting normal brain cognitive function.

Recently, the combination of graph analysis and fMRI offers a powerful tool for characterizing brain networks (Rubinov and Sporns, 2010). Many groups have explored the relationship between the complex topological properties of functional brain networks and cognitive or behavioral measures (Bassett et al., 2009;Crossley et al., 2013;Dosenbach et al., 2007;Hagmann et al., 2010;Lin et al., 2014;van den Heuvel et al., 2009). For example, a recent study has suggested a link between cost and efficiency of complex brain network metrics and working memory cognitive performance (Bassett et al., 2009). Moreover, recent studies show that community structure of the human brain network is relevant to cognitive function (Crossley et al., 2013). These findings further suggest that brain network topology plays an important role in cognitive function.

In addition, brain network functional connectivity is not a static process over time (Allen et al., 2014)***. Emerging evidence suggests that dynamic brain functional connectivity may index changes in neural activity patterns underlying critical aspects of cognition or clinically relevant information (Allen et al., 2014;Calhoun et al., 2014;Hutchison et al., 2013a;Kucyi and Davis, 2015;Park and Friston, 2013;Tagliazucchi and Laufs, 2014;Tagliazucchi et al.,***

2012). Furthermore, understanding the relationship between static and dynamic DMN functional connectivity with brain behaviour will be critical to elucidate more fully the role of DMN signals in both healthy cognition and mental illness (Arenivas et al., 2014;Tam et al., 2014). Despite the number of studies focusing on DMN static and dynamic functional connectivity and mental state, ***TO date, some previous studies have suggested that DMN functional connectivity associated with brain cognitive function (Bonnelle et al., 2012;Buckner et al., 2008;Kucyi and Davis, 2014). However, it still remains unclear how static or dynamic DMN functional connectivity links to cognitive behaviors and mental illness.*** More recent studies indicate that nodal topology properties of brain network associated brain cognitive function and brain disorder(Achard et al., 2012;Buckner et al., 2009). Given that the central PCC region has greater communication with other brain systems, which play an important role in regulating resources competition during attention, and in supporting higher-level executive function tasks (Leech and Sharp, 2013;Liang et al., 2013a), ***we hypothesized that characteristics of resting-state PCC nodal degree would be associated with upcoming task performance. This would suggest that static and dynamic PCC nodal temporal topological properties are linked to underlying behavioural performance.***

Materials and methods

Subjects

Fourteen right-handed subjects ***(6 femals, mean age: 27.4 years, range: 23-35)*** participated in the experiment. All subjects were healthy without a history of neurological or psychiatric episodes. Participants gave written informed consent for a protocol approved by the ethics committee of the University of Trento, Italy.

Experiment Design

In order to explore the resting-state brain network, we run 10 minute (min) resting-state scanning, prior to the task, where subjects were instructed simply to keep their eyes closed and not to think of anything in particular. After this 10 min resting-state scanning, the subjects perform an attention task. See Fig.1 for the task design and timing parameters. The prime stimuli were a square, diamond or star. The primes were followed by an instruction cue (square or diamond) presented at the center of the screen. If the instruction cue shape matched the prime stimuli, this condition would be congruent, if the instruction cue had the opposite shape as the prime stimuli, it would be incongruent; or, if the prime stimuli shape is a star, it would be neutral. The participants were instructed to press the contralateral button if they saw a small central square cue. Alternatively, if they saw a small central diamond cue, participants were required to press the ipsilateral button. For more details about the experimental design of this attention task see our prior published paper (De Pisapia et al., 2012).

MRI data acquisition

Functional images were acquired with a 4-T MRI system (Bruker/Siemens MedSpec, Germany) equipped with a birdcage RF transmit head coil and an eight-channel phase array receiver headcoil. Foam padding and headphones were used to limit head motion and reduce scanner noise. The functional imaging data were acquired using a echo-planar (EPI) sequence, corrected for distortion with the ***point spread function (PSF)*** method (time repetition, TR = 2500 ms; time echo, TE = 33 ms; flip angle, FA = 76°; 3 x 3 x 3 mm voxels; field of view, FOV = 192)

(Zaitsev et al., 2004). Whole-brain coverage including the entire cerebellum was achieved with 33 slices aligned to AC-PC line. Structural images were acquired using a sagittal magnetization prepared rapid gradient echo (MP-RAGE) three-dimensional T1-weighted sequence optimized for gray-white matter contrast (repetition time, TR = 2700 ms, echo time, TE = 4.18 ms, inversion time,TI = 1020 ms, flip angle = 7°, and matrix size = 224×256, 1x1x1 mm3, GRAPPA iPAT = 2).

fMRI Analysis

Data Preprocessing

The functional images were performed by using a combination of analysis of fMRI data based on AFNI (http://afni.nimh.nih.gov/afni/) and FSL's software Library (http://www.fmrib.ox.ac.uk/fsl/). The first five volumes were discarded from analysis to allow for initial stabilization of the fMRI signal. For each subject, motion correction was performed using 3D image realignment with the AFNI program 3dvolreg function, which uses a weighted least squares rigid-body registration algorithm. Each subject's fMRI data was registered to the MNI152 standard template by using FSL's linear registration algorithm (FLIRT) (Smith, Jenkinson et al. 2004). For each subject, the data were spatially smoothed using a Gaussian kernel of ***Full width at half maximum (FWHM)*** 6mm.

Functional Connectivity Analysis

Prior to performing functional connectivity analysis, several processing steps were used to conduct the fMRI data for analysis of voxel-based correlations (Fox et al., 2005). Here, we use temporal band-pass filtering (0.009 Hz<f<0.08Hz) to reduce the effect of low frequency drift and high frequency physiological noise. Several sources of nuisance covariates were eliminated using linear regression: 1) 6 rigid body motion correction parameters, 2) signal from the white matter and the signal from a ventricle region of interest. Recently, the issue of whole-brain signal regression has raised challenging interpretive issues. Further evidence suggests that the BOLD global signal, typically removed as a nuisance term in resting-state studies, may have a neural origin. The use of global signal regression is still under debate as a preprocessing step in resting-state fMRI analysis, and its use is not universally recommended (Murphy et al., 2009;Scholvinck et al., 2010). Here, we do not remove the global whole brain signal.

In the present study, we defined the DMN regions of interest (ROIs) for functional connectivity analysis according to previous studies (Chikazoe et al., 2007;Corbetta and Shulman, 2002;Fair et al., 2008;Konishi et al., 2002;Van Dijk et al., 2010). For each participant resting-state fMRI data, a seed-based correlation analysis was calculated by extracting the BOLD time course from the posterior cingular cortex (PCC). The seed was constructed by forming an 8 mm sphere centered at foci as defined by MNI space (0,-53,26) (Andrews-Hanna et al., 2007;Van Dijk et al., 2010). Then, for each subject, we computed the correlation coefficient between that time course and the time course from all other brain regions. To test for significant connectivity changes in an individual subject, temporal correlation coefficients relative to PCC were converted to z-scores by using Fisher's r-to-z transformation. For group-level statistical significance analysis, we computed a one-sample t-test to determine the regions showing significant functional connectivity with PCC. Finally, group based z-score maps were corrected for multiple comparisons using FWE-corrected for peak voxels; the corrected threshold was set at $P < 0.05$

(see Fig.4). The center of each DMN ROI was determined by considering the coordinates of the z-value local maxima on the correlation map and the DMN ROIs, and then used for the subsequent analysis (see Table 1).

Static and Dynamic Graph Theory Analysis

Using graph theory, functional brain networks can be defined as a graph G=(V,E), with V the collection of nodes reflecting the brain regions, and E the functional connections between these brain regions (Rubinov and Sporns, 2010;Sporns et al., 2000). Most graph measures have only been defined for the simplest case of an unweighted graph; for instance, by setting all edges with a weight above a certain threshold to binary. However, unweighted graph analysis has certain disadvantages. For example, much of the information available in the weights is not used. To understand better the complex brain systems under study, it is evident that information about the nature and strength of the underlying node interactions should be taken into account in order to build the weighted network. A recent study used the weighted graph approach to characterize subtle network changes in mental disease (Castellanos et al., 2010). In addition, a recent study suggested that global network topological properties are not sufficient to describe the mental state of the brain (Achard et al., 2012). For this reason, we only focused on analyzing local nodal degree topological properties. The degree of a node describes the number of connections of a node and provides about the existence of highly connected hub nodes in a brain network. Here, we characterized the static and dynamic complex network nodal topology metric degree of DMN networks by a weighted network analysis approach. Using graph theory, the degree s_i of a node i is the number of edges linking to the node, and is defined as:

$$s_i = \sum_j \omega_{ij} \tag{1}$$

Degree is a simple measurement for the connectivity of a node with the rest of the nodes in a network. The mean of degrees over all the nodes in G, referred to as the average degree, measures the extent to which the graph is connected. The weighted network analysis was based on BCT Matlab toolbox (http://www.brain-connectivity-toolbox.net) (Rubinov and Sporns, 2010) and our own in-house program.

To obtain the static and dynamic nodal degree topological metric of the DMN, we performed the following steps ***(see Fig.3):***

1) Static DMN complex analysis: The mean time series for each DMN ROI was then calculated by taking the mean of the voxel time series within each region. The Pearson's correlation coefficients were computed between each pair of DMN regions for each subject, and then a correlation matrix for each subject was obtained. For further statistical analysis, a Fisher's r-to-z transformation was applied to improve the normality of the correlation coefficients. Then, we set the negative functional connectivity to 0. We further use the weighted graph method to calculate the nodal degree topological metrics of DMN. Then, we characterized the static nodal degree topological metrics of DMN by using a weighted complex network analysis method based on BCT Matlab toolbox.

2) Dynamic DMN complex analysis: first, the mean time series for each DMN ROI was then calculated by taking the mean of the voxel time series with each region. The dynamic pearson's correlation coefficients were computed between all pair of brain regions time series for each subject based on the different sliding window (1min and 2mins) and sliding within a step of one

TR, then the 11×11 dynamic correlation matrix for each subject is obtained. For further statistical analysis, a Fisher's r-to-z transformation is applied to improve the normality of the correlation coefficients. Then, we set the negative functional connectivity to 0. We further use the weighted graph method to calculate the nodal degree topological metrics of DMN. The dynamic correlation matrix for each subject and each sliding window was then obtained base on above analysis. Then, we characterized the dynamic degree topological metrics of DMN for each sliding window by using a weighted complex network analysis method based on BCT Matlab toolbox.

Statistical analysis

To assess task performance differences between reaction times, we performed a paired t-test between each condition. To assess the relation between DMN degree topological properties and behavior we used a robust regression approach (Street et al., 1988) against unrepresentative outliers in the data, as implemented using robust-fit function of the matlab language. Such robust regression methods have been proposed for analysis of brain-behavioral (Marchant and Driver, 2013;van den Bos et al., 2013;Yan et al., 2014).

Results

1. Behavioral Results

Fig.2 shows the mean reaction time for all subjects for the task run sessions for ipsilateral trials including congruent, neutral and incongruent conditions. To assess task performance differences between reaction times, we performed a paired t-test between each condition. A paired t-test indicated that responses were reliably slower in the incongruent ipsilateral condition than the neutral ipsilateral condition (t(13) = -3.5931, p=0.003). The congruent ipsilateral condition was responded to more quickly than to the incongruent ipsilateral condition (t(13) = -2.65, p=0.02). There were no significant differences found for contralateral trials including congruent, neutral and incongruent conditions (p>0.05).

2. DMN Functional Connectivity Mapping

Fig.4 shows the group functional connectivity z-map of the PCC seed after correcting for multiple comparisons using FWE-corrected for peak voxels; the corrected threshold was set at $P < 0.05$. ***Eleven regions of the DMN (see Table.1), which were considered for DMN graph analysis.***

3 . Static Resting-State PCC Nodal Degree and Behavioral Performance

To explore a more detailed understanding of the relationship between PCC and the MPFC key regional nodal topology and behavioral performance, we correlated, in individual subjects, the nodal level topological properties of PCC, dmPFC and vmPFC and reaction time in the attention task. We found that degree of the PCC region, alone, showed a significant negative correlation with RT task performance, in the congruent ipsilateral, incongruent ipsilateral, incongruent contralateral and neutral ipsilateral conditions. Here, PCC degree correlated with reaction time in the congruent ipsilateral condition (p=0.028,R2 = 0.36, Fig. 5A), the neutral ipsilateral condition (p= 0.04, R2= 0.32, Fig. 5B), the incongruent ipsilateral condition (p=0.04, R2= 0.34) and the incongruent contralateral condition (p= 0.02, R2= 0.37, Fig. 5C). We did not observe significant correlation between congruent contralateral, neutral contralateral and reaction time (p>0.05).

We observed a robust negative correlation between PCC degree and and reaction time, suggesting that higher PCC nodal degree is associated with shorter reaction time. In addition, we further analyzed the relationship between task performance and nodal degree in two core DMN regions, the vmPFC and dmPFC (see Fig.6). In contrast, for these regions, we did not find significant correlations between node degree and reaction time. The other DMN sub region degree also did not associated with task performance (Supplementary Table S1).

4. Dynamic Resting-State PCC Nodal Degree and Behavioral Performance

To explore the underlying relationship between dynamic DMN nodal topology and behavioral performance, we correlated, in individual subjects, dynamic nodal level topological properties and the attention task reaction time. The effect of window length on DMN topology is significant, the shorter window lengths measure for dynamic FC normally used shorter sliding window length (60s) (Allen et al., 2014;Chang and Glover, 2010;Handwerker et al., 2012). Therefore, we focus on the shorter sliding window length (1min) dynamics analysis. The mean and variance of time-evolving PCC degree across different subjects is illustrated in Fig.7A. Fig.7B illustrates the association between RT and mean PCC dynamic degree values for incongruent ipsilateral ($p=0.048$, $R2= 0.34$) and incongruent contralateral ($p= 0.04$, $R2= 0.36$) conditions. In order to fully extract the addition information provided by the dynamic measure, we further investigate the relationship between RT and variance of PCC dynamic degree. Fig.7C illustrates the association between RT and variance of PCC dynamic degree for incongruent ipsilateral ($p=0.048$, $R2= 0.13$) and incongruent contralateral ($p= 0.004$, $R2= 0.1$) conditions.

Here, we found the dynamic mean values of PCC nodal degree negative correlated with RT. Higher degree are consistent with faster RT. Specifically, the variance of dynamic PCC nodal degree shows positive correlated with RT. However, we did not observe the significant correlation between PCC dynamic degree and RT within other condition (congruent ipsilateral, congruent contralateral, neutral contralateral and neutral ipsilateral) (Supplementary Fig.S1).

Next, we focus on the longer sliding window length (2mins) dynamics analysis. The mean and variance of time-evolving PCC degree across different subjects is illustrated in Fig.8A. Fig.8B illustrates the association between RT and average values of PCC dynamic degree for incongruent ipsilateral ($p=0.03$, $R2= 0.35$) and incongruent contralateral ($p= 0.02$, $R2= 0.4$). Fig.8C illustrates the association between RT and variance of PCC dynamic degree for incongruent ipsilateral ($p=0.03$, $R2= 0.28$) and incongruent contralateral ($p= 0.01$, $R2= 0.3$) conditions. No significant correlation was found within other condition (Supplementary Fig.S2). In contrast, for other DMN region, we did not find stable and significant correlation between dynamic nodal degree and reaction time during time-sliding window analysis (Supplementary Table S2-S5).

Discussion

The resting-state brain network is a complex dynamic network in which information is continuously processed and transported between spatially distributed but functionally linked sub-networks or regions. However, the function of intrinsic resting-state DMN activity remains poorly understood without being able to show a clear-cut brain-behavior relationship. How this resting-state DMN organization is related to cognitive behavioral performance remains an open question. To address this question, we investigated the relationship between DMN nodal topological properties and behavioral performance. We found that PCC nodal degree significantly correlated with task reaction time. Our results suggest that brain network nodal topological properties, in fact, do link to brain behavioral performance.

Static PCC Nodal Topology and Behavioral Performance

Recent studies suggest that whole network topological metrics are not sufficient to characterize cognitive behavioral performance (Achard et al., 2012). The network topology can also be estimated from each individual node in the brain network, thus allowing a more refined analysis of changes in brain function associated with behavioral performance. More importantly, the local topological features, such as DMN PCC node, are likely to be more important in understanding human cognitive behavior (Leech and Sharp, 2013;Power et al., 2013).We calculated the correlation between nodal topology and behavioral response times. We found that PCC nodal degree shows a significant negative correlation with task reaction times in the incongruent ipsilateral and incongruent contralateral conditions.

As expected, we found the degree of the PCC node predicts task performance in an attention task. The PCC node may play an important role to support the higher communication rate within the DMN (Buckner et al., 2008;Utevsky et al., 2014). Evidence from functional studies of brain DMN development have demonstrated age-related increases in connection strength within the DMN and in functional integration of the initial subsystems into a more coherent network (Supekar et al., 2009;Supekar et al., 2010). Furthermore, DTI-based studies show that the PCC is a hub region that widely connects with other DMN regions (Gong et al., 2009). Our results show PCC-degree negatively correlated with the incongruent condition reaction time. A variety of studies have proved that the high interference during the incongruent condition is associated with a longer RT (Kucyi and Davis, 2015;Sharp et al., 2011).

In line with previous studies, processing efficiency during interference related tasks is correlated with degree of DMN activity (De Pisapia et al., 2012;Weissman et al., 2006). This longer reaction time during the incongruent condition, in turn, the production of less PCC deactivation (Weissman et al., 2006). Accumulating evidences indicate efficient behavior was associated with increased PCC deactivation or its functional connectivity (Leech et al., 2011;Leech and Sharp, 2013). Further studies show that greater PCC deactivation is associated with higher amount of focused attention resource compared with a low-level difficult task condition (De Pisapia et al., 2012;Mantini and Vanduffel, 2013;Marchant and Driver, 2013). Our results show higher PCC nodal degree associated with faster reaction time.

One possible interpretation of these results is that stronger anatomical and functional connectivity probably permits more efficient communication among DMN regions for the support of incongruent task performance. Our results may indicate that higher PCC node degree enables efficient information flow across the whole DMN and, thus, facilitates integrative information processing speed during the incongruent condition compared with the congruent condition. Increased PCC deactivation in the DMN typically indexes more effortful processing and it is associated with increased task difficulty (McKiernan et al., 2003). Thus, we can expect that PCC play less effortful processing during less task stimuli condition, such as congruent and neutral condition. For example, previous studies have suggest that the level of PCC deactivations during incongruent condition is significantly higher compared to neutral and congruent condition (De Pisapia et al., 2012). Furthermore, PCC functional connectivity correlating with the task performance of cognitive processing in various cognitive tasks (Kucyi and Davis, 2014;Leech and Sharp, 2013;Liang et al., 2013a). For example, recent studies show that increased functional connectivity of the PCC within the DMN is correlated with faster reaction times to external task stimuli in both healthy and traumatic brain injury subjects (Bonnelle et al., 2012;Sharp et al., 2014). Our results further demonstrate that the degree of functional integration within the PCC node could influence ongoing cognitive behavior.

More importantly, recently studies have reported the PCC node consistently exhibits the highest cerebral blood flow (CBF) and cerebral metabolism rate for oxygen (CMRO2) during the resting-state (Pfefferbaum et al., 2011a;Pfefferbaum et al., 2011b;Raichle and Gusnard, 2002;Raichle et al., 2001), and baseline CBF may be relevant to individual deactivation variability during task performance. Our results highlight the important link of PCC nodal topology and brain behavior. Further, structural connectivity studies indicate that brain spontaneous fluctuations are thought to stem from anatomical connectivity (Greicius et al., 2009;van den Heuvel et al., 2008). For example, structural connectivity brain studies have reported that fractional anisotropy of the posterior cingulum bundle correlated with reaction time task performance (Tam et al., 2014). These studies provide further evidence that brain network activity is coordinated by the PCC and relies on the structural integrity of its white matter connections.

Taken together, previous functional connectivity and structural connectivity studies both support that PCC is the DMN core region, which facilitates information integration within the entire DMN and, thus, aids in ongoing behavioral performance.

Dynamic PCC Nodal Topology and Behavioral Performance

Brain network functional connectivity is not a static process over time (Allen et al., 2014;Chang and Glover, 2010;Chen et al., 2013;Cocchi et al., 2011;Handwerker et al., 2012;Hutchison et al., 2013a;Hutchison et al., 2013b;Kucyi et al., 2013;Lee et al., 2013;Leonardi et al., 2013;Tagliazucchi and Laufs, 2014;Tagliazucchi et al., 2012;Thompson et al., 2013). As dynamic brain network functional connectivity may carry important, cognitive and clinically relevant information (Allen et al., 2014;Hellyer et al., 2014;Ma et al., 2014;Mayhew et al., 2013), in order better to understand dynamic brain network functional connectivity and cognition over time, it is necessary to investigate the relationship between dynamic functional connectivity and brain behavior. Emerging evidence suggests that dynamic brain network or functional connectivity may index changes in neural activity patterns underlying critical aspects of cognition and clinically relevant information (Allen et al., 2014;Hutchison et al., 2013a;Hutchison et al., 2013b). Growing interest in these dynamic networks as a new approach with which to understand information processing across different brain states (task or resting-state), brain development, and disease states, should show a complex and dynamic pattern associated with brain cognition.

PCC is a key cortical region within the DMN system that is involved in several higher brain cognitive functions (Buckner et al., 2008;Leech and Sharp, 2013). To better understand how

PCC activity dynamic changes in resting-state and its association with ongoing brain cognitive function, one very useful and simple approach is to characterize the dynamic PCC node properties during different brain mental states. Dynamic PCC node topology properties of resting-state function brain activity can account for individual task performance differences in several cognitive functions. Dynamic functional connectivity is associated with internal mental state during rest or task states (Fornito et al., 2012). Recently, characterization of the dynamic resting-state network properties has received great interest for the study of DMN neural mechanisms (Chang and Glover, 2010). However, what remains unclear is the key issue of how the DMN organization dynamic configuration links to task performance. Here, we conducted a robust regression, between dynamic PCC node degree and attention cognitive task performance and we observe that DMN PCC dynamic nodal topology property changes are associated with task performance. We found the mean dynamic degree robust negative correlated with RT across incongruent ipsilateral and incongruent contralateral. One possible explain is that higher PCC degree indicate more efficient information transfer performance within brain for support higher difficult ongoing task (Liang et al., 2013b). We also found the variance values of dynamic degree stable positive correlated with RT across incongruent ipsilateral and incongruent contralateral. Our results show that PCC nodal topological properties variability link to task performance. In particular, emerging evidence suggests that brain region variability correlated with task performance (Calhoun et al., 2014;Kucyi and Davis, 2015;Lin et al., 2014). Furthermore, one previous study found that dynamic DMN FC variability reflects the degree of ongoing mind-wandering (Kucyi and Davis, 2014). The DMN sub-regions show decreasing variability activity for support external task stimuli (Garrett et al., 2011;Liang et al., 2013b).

This evidence indicates that higher mind-wandering ratio would link to worst task performance during task stimuli (Kucyi and Davis, 2014). Inverse, lower mind-wandering ratio would link to better task performance. Further work is needed to uncover the potential relationship between dynamic mind-wandering ratio, PCC nodal topology and task performance.

Our results suggest the important role that the dynamic temporal-topological structure of the PCC hub within the DMN may play in brain adaptive information processing and cognitive integration. Furthermore, the topological structure of PCC node degree shows dynamic change over time. The observed dynamic topological structure of PCC could represent a brain microstate temporal signature for supporting internal and ongoing different brain state cognitive ***processes (Kucyi and Davis, 2014;Kucyi and Davis, 2015)***; especially, the dynamic topological properties of PCC correlated with task performance during an attention task. Our results suggest that PCC node temporal topological structure dynamically changes during different brain resting-state microstates in order to support ongoing brain information processing.

In addition, of note, a new finding in our research is that PCC is the only core region within the DMN, which stably correlated with cognitive task performance. The PCC may be the key node to which information converges allowing for functional cooperation within the DMN. Here, our findings strongly indicate that the dynamic PCC node communication structure within the DMN is associated with cognitive function, which can support a variety of task performance. More importantly, our results suggest that the PCC node plays a critical role for coordinating brain network information communication in order to support cognition function.

Limitations

There were a number of limitations in our study. First , in this study, we only use one attention cognitive task. Therefore, it will be important for future studies to collect both behavioral and multiple cognitive tasks imaging data to understand the relationship between different cognitive task performance and DMN topological metric. Second, we used traditional BOLD fMRI which temporal resolution is not enough high to capture the underling dynamics information. In our future work, we intend to study brain network dynamics using faster neuroimag techniques such as electroencephalography (EEG), magnetoencephalography (MEG)and multi-band imaging. More important, the combination of fMRI-EEG method can provide better understanding of the dynamic functional connectivity in humans across multiple cognitive tasks

Conclusions

In conclusion, this study shows that there is a relationship between static, intrinsic resting-state DMN brain network activity and cognitive behavior. Our results show that the resting-state PCC nodal degree is significantly associated with task performance. In addition, the dynamic PCC nodal degree is also related to task performance. Our findings suggest the important link between both static and dynamic PCC region temporal topological properties and underlying brain cognition and adaptive information processing function. Future studies of PCC nodal topology properties will continue to be highly important for greater understanding of brain function and brain disorders.

Acknowledgments

Government of the Provincia Autonoma di Trento, Italy, Project PAT Post-doc 2006; Fondazione Cassa di Risparmio di Trento e Rovereto; and University of Trento, Italy. This work was supported by the National Natural Science Foundation of China (61473221,61262034), by Doctoral Fund of Ministry of Education of China (20120201120071), by the Fundamental Research Funds for the Central Universities of China.

Competing interests

The authors declare that we have no competing financial interests.

Informed Consent

All procedures followed were in accordance with the ethical standards of the responsible committee on human experimentation (institutional and national) and with the Helsinki Declaration of 1975, and the applicable revisions at the time of the investigation. Informed consent was obtained from all patients for being included in the study.

References

Achard S, Delon-Martin C, Vertes PE, Renard F, Schenck M, Schneider F, Heinrich C, Kremer S, Bullmore ET. 2012. Hubs of brain functional networks are radically reorganized in comatose patients. Proc Natl Acad Sci U S A 109(50):20608-13.

Allen EA, Damaraju E, Plis SM, Erhardt EB, Eichele T, Calhoun VD. 2014. Tracking whole-brain connectivity dynamics in the resting state. Cereb Cortex 24(3):663-76.

Andrews-Hanna JR, Snyder AZ, Vincent JL, Lustig C, Head D, Raichle ME, Buckner RL. 2007. Disruption of large-scale brain systems in advanced aging. Neuron 56(5):924-935.

Arenivas A, Diaz-Arrastia R, Spence J, Cullum CM, Krishnan K, Bosworth C, Culver C, Kennard B, Marquez de la Plata C. 2014. Three approaches to investigating functional compromise to the default mode network after traumatic axonal injury. Brain Imaging and Behavior 8(3):407-19.

Bassett DS, Bullmore ET, Meyer-Lindenberg A, Apud JA, Weinberger DR, Coppola R. 2009. Cognitive fitness of cost-efficient brain functional networks. Proceedings of the National Academy of Sciences of the United States of America 106(28):11747-52.

Bonnelle V, Ham TE, Leech R, Kinnunen KM, Mehta MA, Greenwood RJ, Sharp DJ. 2012. Salience network integrity predicts default mode network function after traumatic brain injury. Proc Natl Acad Sci U S A 109(12):4690-5.

Buckner RL, Andrews-Hanna JR, Schacter DL. 2008. The brain's default network: anatomy, function, and relevance to disease. Ann N Y Acad Sci 1124:1-38.

Buckner RL, Sepulcre J, Talukdar T, Krienen FM, Liu HS, Hedden T, Andrews-Hanna JR, Sperling RA, Johnson KA. 2009. Cortical Hubs Revealed by Intrinsic Functional Connectivity: Mapping, Assessment of Stability, and Relation to Alzheimer's Disease. Journal of Neuroscience 29(6):1860-1873.

Calhoun VD, Miller R, Pearlson G, Adali T. 2014. The Chronnectome: Time-Varying Connectivity Networks as the Next Frontier in fMRI Data Discovery. Neuron 84(2):262-274.

Castellanos NP, Paul N, Ordonez VE, Demuynck O, Bajo R, Campo P, Bilbao A, Ortiz T, del-Pozo F, Maestu F. 2010. Reorganization of functional connectivity as a correlate of cognitive recovery in acquired brain injury. Brain : a journal of neurology 133(Pt 8):2365-81.

Chang C, Glover GH. 2010. Time-frequency dynamics of resting-state brain connectivity measured with fMRI. Neuroimage 50(1):81-98.

Chen JL, Ros T, Gruzelier JH. 2013. Dynamic changes of ICA-derived EEG functional connectivity in the resting state. Human Brain Mapping 34(4):852-868.

Chikazoe J, Konishi S, Asari T, Jimura K, Miyashita Y. 2007. Activation of right inferior frontal gyrus during response inhibition across response modalities. Journal of Cognitive Neuroscience 19(1):69-80.

Cocchi L, Zalesky A, Toepel U, Whitford TJ, De-Lucia M, Murray MM, Carter O. 2011. Dynamic changes in brain functional connectivity during concurrent dual-task performance. PLoS One 6(11):e28301.

Corbetta M, Shulman GL. 2002. Control of goal-directed and stimulus-driven attention in the brain.

Nature Reviews Neuroscience 3(3):201-15.

Crossley NA, Mechelli A, Vertes PE, Winton-Brown TT, Patel AX, Ginestet CE, McGuire P, Bullmore ET. 2013. Cognitive relevance of the community structure of the human brain functional coactivation network. Proc Natl Acad Sci U S A 110(28):11583-8.

De Pisapia N, Turatto M, Lin P, Jovicich J, Caramazza A. 2012. Unconscious priming instructions modulate activity in default and executive networks of the human brain. Cereb Cortex 22(3):639-49.

Dosenbach NUF, Fair DA, Miezin FM, Cohen AL, Wenger KK, Dosenbach RAT, Fox MD, Snyder AZ, Vincent JL, Raichle ME and others. 2007. Distinct brain networks for adaptive and stable task control in humans. Proceedings of the National Academy of Sciences of the United States of America 104(26):11073-8.

Fair DA, Cohen AL, Dosenbach NUF, Church JA, Miezin FM, Barch DM, Raichle ME, Petersen SE, Schlaggar BL. 2008. The maturing architecture of the brain's default network. Proceedings of the National Academy of Sciences of the United States of America 105(10):4028-32.

Fornito A, Harrison BJ, Zalesky A, Simons JS. 2012. Competitive and cooperative dynamics of large-scale brain functional networks supporting recollection. Proc Natl Acad Sci U S A 109(31):12788-93.

Fox MD, Snyder AZ, Vincent JL, Corbetta M, Van Essen DC, Raichle ME. 2005. The human brain is intrinsically organized into dynamic, anticorrelated functional networks. Proceedings of the National Academy of Sciences of the United States of America 102(27):9673-9678.

Garrett DD, Kovacevic N, McIntosh AR, Grady CL. 2011. The Importance of Being Variable. Journal of Neuroscience 31(12):4496-4503.

Gong G, He Y, Concha L, Lebel C, Gross DW, Evans AC, Beaulieu C. 2009. Mapping anatomical connectivity patterns of human cerebral cortex using in vivo diffusion tensor imaging tractography. Cerebral cortex (New York, N Y : 1991) 19(3):524-36.

Greicius MD, Krasnow B, Reiss AL, Menon V. 2003. Functional connectivity in the resting brain: a network analysis of the default mode hypothesis. Proceedings of the National Academy of Sciences of the United States of America 100(1):253-8.

Greicius MD, Supekar K, Menon V, Dougherty RF. 2009. Resting-state functional connectivity reflects structural connectivity in the default mode network. Cerebral cortex (New York, N Y : 1991)

19(1):72-8.

Hagmann P, Sporns O, Madan N, Cammoun L, Pienaar R, Wedeen VJ, Meuli R, Thiran JP, Grant PE. 2010. White matter maturation reshapes structural connectivity in the late developing human brain. Proceedings of the National Academy of Sciences of the United States of America 107(44):19067-72.

Handwerker DA, Roopchansingh V, Gonzalez-Castillo J, Bandettini PA. 2012. Periodic changes in fMRI connectivity. Neuroimage 63(3):1712-9.

Hellyer PJ, Shanahan M, Scott G, Wise RJ, Sharp DJ, Leech R. 2014. The control of global brain dynamics: opposing actions of frontoparietal control and default mode networks on attention. Journal of Neuroscience 34(2):451-61.

Hutchison RM, Womelsdorf T, Allen EA, Bandettini PA, Calhoun VD, Corbetta M, Penna S, Duyn JH, Glover GH, Gonzalez-Castillo J and others. 2013a. Dynamic functional connectivity: Promise, issues, and interpretations. Neuroimage 80:360-378.

Hutchison RM, Womelsdorf T, Gati JS, Everling S, Menon RS. 2013b. Resting-state networks show dynamic functional connectivity in awake humans and anesthetized macaques. Human Brain Mapping 34(9):2154-2177.

Kelly AMC, Uddin LQ, Biswal BB, Castellanos FX, Milham MP. 2008. Competition between functional brain networks mediates behavioral variability. Neuroimage 39(1):527-537.

Konishi S, Hayashi T, Uchida I, Kikyo H, Takahashi E, Miyashita Y. 2002. Hemispheric asymmetry in human lateral prefrontal cortex during cognitive set shifting. Proceedings of the National Academy of Sciences of the United States of America 99(11):7803-8.

Kucyi A, Davis KD. 2014. Dynamic functional connectivity of the default mode network tracks daydreaming. Neuroimage 100:471-80.

Kucyi A, Davis KD. 2015. The dynamic pain connectome. Trends Neurosci 38(2):86-95.

Kucyi A, Salomons TV, Davis KD. 2013. Mind wandering away from pain dynamically engages antinociceptive and default mode brain networks. Proceedings of the National Academy of Sciences of the United States of America 110(46):18692-18697.

Lee HL, Zahneisen B, Hugger T, Levan P, Hennig J. 2013. Tracking dynamic resting-state networks at higher frequencies using MR-encephalography. Neuroimage 65:216-222.

Leech R, Kamourieh S, Beckmann CF, Sharp DJ. 2011. Fractionating the default mode network: distinct contributions of the ventral and dorsal posterior cingulate cortex to cognitive control. Journal of Neuroscience 31(9):3217-24.

Leech R, Sharp DJ. 2013. The role of the posterior cingulate cortex in cognition and disease. Brain.

Leonardi N, Richiardi J, Gschwind M, Simioni S, Annoni JM, Schluep M, Vuilleumier P, Van De Ville D. 2013. Principal components of functional connectivity: a new approach to study dynamic brain connectivity during rest. Neuroimage 83:937-50.

Liang X, Zou Q, He Y, Yang Y. 2013a. Coupling of functional connectivity and regional cerebral blood flow reveals a physiological basis for network hubs of the human brain. Proc Natl Acad Sci U S A 110(5):1929-34.

Liang X, Zou QH, He Y, Yang YH. 2013b. Coupling of functional connectivity and regional cerebral blood flow reveals a physiological basis for network hubs of the human brain. Proceedings of the National Academy of Sciences of the United States of America 110(5):1929-1934.

Lin P, Hasson U, Jovicich J, Robinson S. 2011. A neuronal basis for task-negative responses in the human brain. Cerebral cortex (New York, N Y : 1991) 21(4):821-30.

Lin P, Sun JB, Yu G, Wu Y, Yang Y, Liang ML, Liu X. 2014. Global and local brain network reorganization in attention-deficit/hyperactivity disorder. Brain Imaging and Behavior 8(4):558-569.

Ma S, Calhoun VD, Phlypo R, Adali T. 2014. Dynamic changes of spatial functional network connectivity in healthy individuals and schizophrenia patients using independent vector analysis. Neuroimage 90:196-206.

Mantini D, Vanduffel W. 2013. Emerging roles of the brain's default network. Neuroscientist 19(1):76-87.

Marchant JL, Driver J. 2013. Visual and audiovisual effects of isochronous timing on visual perception and brain activity. Cereb Cortex 23(6):1290-8.

Mayhew SD, Hylands-White N, Porcaro C, Derbyshire SWG, Bagshaw AP. 2013. Intrinsic variability in the human response to pain is assembled from multiple, dynamic brain processes. Neuroimage 75:68-78.

McKiernan KA, Kaufman JN, Kucera-Thompson J, Binder JR. 2003. A parametric manipulation of factors affecting task-induced deactivation in functional neuroimaging. Journal of Cognitive Neuroscience 15(3):394-408.

Murphy K, Birn RM, Handwerker DA, Jones TB, Bandettini PA. 2009. The impact of global signal regression on resting state correlations: Are anti-correlated networks introduced? Neuroimage 44(3):893-905.

Park HJ, Friston K. 2013. Structural and functional brain networks: from connections to cognition. Science 342(6158):1238411.

Patel KT, Stevens MC, Pearlson GD, Winkler AM, Hawkins KA, Skudlarski P, Bauer LO. 2013. Default mode network activity and white matter integrity in healthy middle-aged ApoE4 carriers. Brain Imaging and Behavior 7(1):60-67.

Pfefferbaum A, Chanraud S, Pitel AL, Muller-Oehring E, Shankaranarayanan A, Alsop DC, Rohlfing T, Sullivan EV. 2011a. Cerebral blood flow in posterior cortical nodes of the default mode network decreases with task engagement but remains higher than in most brain regions. Cereb Cortex 21(1):233-44.

Pfefferbaum A, Chanraud S, Pitel AL, Muller-Oehring E, Shankaranarayanan A, Alsop DC, Rohlfing T, Sullivan EV. 2011b. Cerebral blood flow in posterior cortical nodes of the default mode network decreases with task engagement but remains higher than in most brain regions. Cerebral cortex (New York, N Y : 1991) 21(1):233-44.

Philip NS, Sweet LH, Tyrka AR, Price LH, Carpenter LL, Kuras YI, Clark US, Niaura RS. 2013. Early life stress is associated with greater default network deactivation during working memory in healthy controls: a preliminary report. Brain Imaging and Behavior 7(2):204-212.

Power JD, Schlaggar BL, Lessov-Schlaggar CN, Petersen SE. 2013. Evidence for hubs in human functional brain networks. Neuron 79(4):798-813.

Raichle ME, Gusnard DA. 2002. Appraising the brain's energy budget. Proceedings of the National Academy of Sciences of the United States of America 99(16):10237-9.

Raichle ME, MacLeod AM, Snyder AZ, Powers WJ, Gusnard DA, Shulman GL. 2001. A default mode of brain function. Proc Natl Acad Sci U S A 98(2):676-82.

Rubinov M, Sporns O. 2010. Complex network measures of brain connectivity: uses and interpretations. Neuroimage 52(3):1059-69.

Scholvinck ML, Maier A, Ye FQ, Duyn JH, Leopold DA. 2010. Neural basis of global resting-state fMRI activity. Proceedings of the National Academy of Sciences of the United States of America 107(22):10238-43.

Sharp DJ, Beckmann CF, Greenwood R, Kinnunen KM, Bonnelle V, De Boissezon X, Powell JH, Counsell SJ, Patel MC, Leech R. 2011. Default mode network functional and structural connectivity after traumatic brain injury. Brain 134(Pt 8):2233-47.

Sharp DJ, Scott G, Leech R. 2014. Network dysfunction after traumatic brain injury. Nat Rev Neurol 10(3):156-66.

Sporns O, Tononi G, Edelman GM. 2000. Theoretical neuroanatomy: Relating anatomical and functional connectivity in graphs and cortical connection matrices. Cerebral Cortex 10(2):127-141.

Street JO, Carroll RJ, Ruppert D. 1988. A Note on Computing Robust Regression Estimates Via Iteratively Reweighted Least-Squares. American Statistician 42(2):152-154.

Supekar K, Musen M, Menon V. 2009. Development of large-scale functional brain networks in children. PLoS biology 7(7):e1000157.

Supekar K, Uddin LQ, Prater K, Amin H, Greicius MD, Menon V. 2010. Development of functional and structural connectivity within the default mode network in young children. Neuroimage 52(1):290-301.

Tagliazucchi E, Laufs H. 2014. Decoding Wakefulness Levels from Typical fMRI Resting-State Data Reveals Reliable Drifts between Wakefulness and Sleep. Neuron 82(3):695-708.

Tagliazucchi E, von Wegner F, Morzelewski A, Brodbeck V, Laufs H. 2012. Dynamic BOLD functional connectivity in humans and its electrophysiological correlates. Front Hum Neurosci 6:339.

Tam A, Luedke AC, Walsh JJ, Fernandez-Ruiz J, Garcia A. 2014. Effects of reaction time variability and age on brain activity during Stroop task performance. Brain Imaging and Behavior.

Thompson GJ, Merritt MD, Pan WJ, Magnuson ME, Grooms JK, Jaeger D, Keilholz SD. 2013. Neural correlates of time-varying functional connectivity in the rat. Neuroimage 83:826-36.

Utevsky AV, Smith DV, Huettel SA. 2014. Precuneus Is a Functional Core of the Default-Mode Network. Journal of Neuroscience 34(3):932-940.

van den Bos W, Talwar A, McClure SM. 2013. Neural correlates of reinforcement learning and social preferences in competitive bidding. Journal of Neuroscience 33(5):2137-46.

van den Heuvel M, Mandl R, Luigjes J, Hulshoff Pol H. 2008. Microstructural organization of the cingulum tract and the level of default mode functional connectivity. J Neurosci 28(43):10844-51.

van den Heuvel MP, Stam CJ, Kahn RS, Hulshoff Pol HE. 2009. Efficiency of functional brain networks and intellectual performance. The Journal of neuroscience : the official journal of the Society for Neuroscience 29(23):7619-24.

Van Dijk KRA, Hedden T, Venkataraman A, Evans KC, Lazar SW, Buckner RL. 2010. Intrinsic Functional Connectivity As a Tool For Human Connectomics: Theory, Properties, and Optimization. Journal of Neurophysiology 103(1):297-321.

van Veluw SJ, Chance SA. 2014. Differentiating between self and others: an ALE meta-analysis of fMRI studies of self-recognition and theory of mind. Brain Imaging and Behavior 8(1):24-38.

Weissman DH, Roberts KC, Visscher KM, Woldorff MG. 2006. The neural bases of momentary lapses in attention. Nature Neuroscience 9(7):971-8.

Yan Y, Rasch MJ, Chen M, Xiang X, Huang M, Wu S, Li W. 2014. Perceptual training continuously refines neuronal population codes in primary visual cortex. Nat Neurosci 17(10):1380-7.

Zaitsev M, Hennig J, Speck O. 2004. Point spread function mapping with parallel imaging techniques and high acceleration factors: Fast, robust, and flexible method for echo-planar imaging distortion correction. Magnetic Resonance in Medicine 52(5):1156-1166.

Table.1 Definition of DMN seed regions

Region	Abbreviation	MNI coordinates		
		X	Y	Z
Posterior cingulate cortex	PCC	0	-53	26
dorsal Medial prefrontal Cortex	dmPFC	-3	55	22
ventral Medial prefrontal Cortex	vmPFC	-3	59	-7
Left Parahippocampal Gyus	LPHG	-24	-33	-27
Right Parahippocampal Gyrus	RPHG	30	-33	-27
Left Lateral parietal cortex	LLP	-52	-69	26
Right Lateral parietal cortex	RLP	48	- 67	36
Left superior frontal cortex	LSupF	-21	32	47
Right superior frontal cortex	RSupF	12	44	48
Left inferior Temporal cortex	LITC	-61	-17	-30
Right inferior Temporal cortex	RITC	61	-5	-25

Figure Legends

Figure 1. Experiment design. (A) Task design order: pre resting-state and attention task. For rest conditions, subjects were instructed to lie still, relaxed, and with eyes close. For the cognitive task condition, subjects performed attention task. (B) Attention task design.

Figure 2. Behavioral Results: Mean RTs (±s.e.m.) across conditions for incongruent ipsilateral , neutral ipsilateral and congruent ipsilateral condition.A paired t-test indicated that responses were reliably slower in the incongruent ipsilateral condition than the neutral ipsilateral condition (t(13) = -3.5931, p=0.003). The congruent ipsilateral condition were responded to more quickly than incongruent ipsilateral condition (t(13) = -2.65, p=0.02). Note: CongIpsi-congruent= ipsilateral;NeuIpsi-neutral= ipsilateral;IncIpsi- incongruent= ipsilateral.

Figure 3. Analysis schematic. (A) Static DMN complex analysis .(B) Dynamic DMN complex analysis.

Figure 4. Group functional connectivity mapping of the posterior cingulate cortex during rest (cluster-level FWE-corrected $p<0.05$)

Figure 5. Relationship between PCC nodal topological metric and behavioral performance during attention task. Scatterplots of the association between task reaction time and PCC mean degree values. (A) shows the association between RT and PCC mean degree values for congruent ipsilateral ($p=0.028, R^2 = 0.36$) and congruent contralateral ($p=0.057$, $R^2= 0.28$); (B) shows the association between RT and PCC mean degree values for neutral ipsilateral ($p=0.08$, $R^2= 0.26$) and neutral contralateral ($p= 0.04$, $R^2= 0.32$). (C) shows the association between RT and PCC mean degree values for incongruent ipsilateral ($p=0.04$, $R^2= 0.34$) and incongruent contralateral ($p= 0.02$, $R^2= 0.37$).

Figure 6. Relationship between brain–network metrics and behavioral performance. Scatterplots of the association between reaction time and dmPFC and vnPFC mean degree values. No

significant correlation between them was observed ($p>0.05$).

Figure 7. The relationship between dynamic resting-state DMN PCC degree and task performance based on 1 min sliding window analysis. (A) The mean dynamic time-evolving PCC degree topological properties within 14 subjects across the whole resting state period. (B) The association between RT and PCC dynamic degree values for incongruent ipsilateral ($p=0.048$, $R^2= 0.34$) and incongruent contralateral ($p= 0.04$, $R^2=0.36$). (C) The association between RT and variance of PCC dynamic degree for incongruent ipsilateral ($p=0.048$, $R^2= 0.13$) and incongruent contralateral ($p= 0.004$, $R^2= 0.1$). Shaded regions indicate standard error.

Figure 8. The relationship between dynamic resting-state DMN PCC degree and task performance based on 2 min sliding window analysis. (A) The mean dynamic time-evolving PCC degree topological properties within 14 subjects across the whole resting state period. (B) The association between RT and PCC dynamic degree values for incongruent ipsilateral ($p=0.03$, $R^2= 0.35$) and incongruent contralateral ($p= 0.02$, $R^2=0.4$). (C) The association between RT and variance of PCC dynamic degree for incongruent ipsilateral ($p=0.03$, $R^2= 0.28$) and incongruent contralateral ($p= 0.01$, $R^2= 0.3$). Shaded regions indicate standard error.

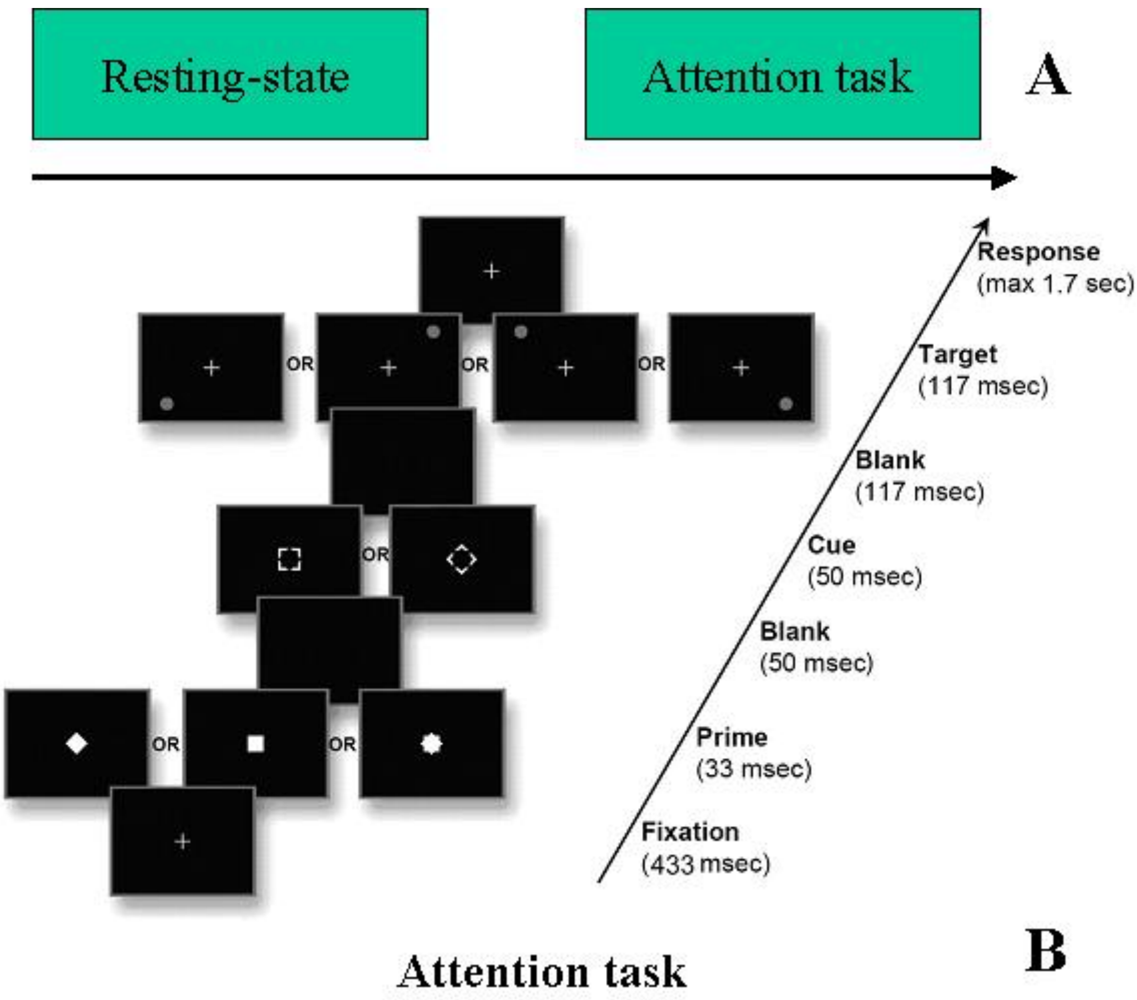

Figure 1. Experiment design. (A) Task design order: pre resting-state and attention task. For rest conditions, subjects were instructed to lie still, relaxed, and with eyes close. For the cognitive task condition, subjects performed attention task. (B) Attention task design: The prime stimuli were a square, diamond or star. The primes were followed by an instruction cue (square or diamond) presented at the center of the screen. If the instruction cue shape matched the prime stimuli, this condition would be congruent, if the instruction cue had the opposite shape as the prime stimuli, it would be incongruent; or, if the prime stimuli shape is a star, it would be neutral. The participants were instructed to press the contralateral button if they saw a small central square cue. Alternatively, if they saw a small central diamond cue, participants were required to press the ipsilateral button.

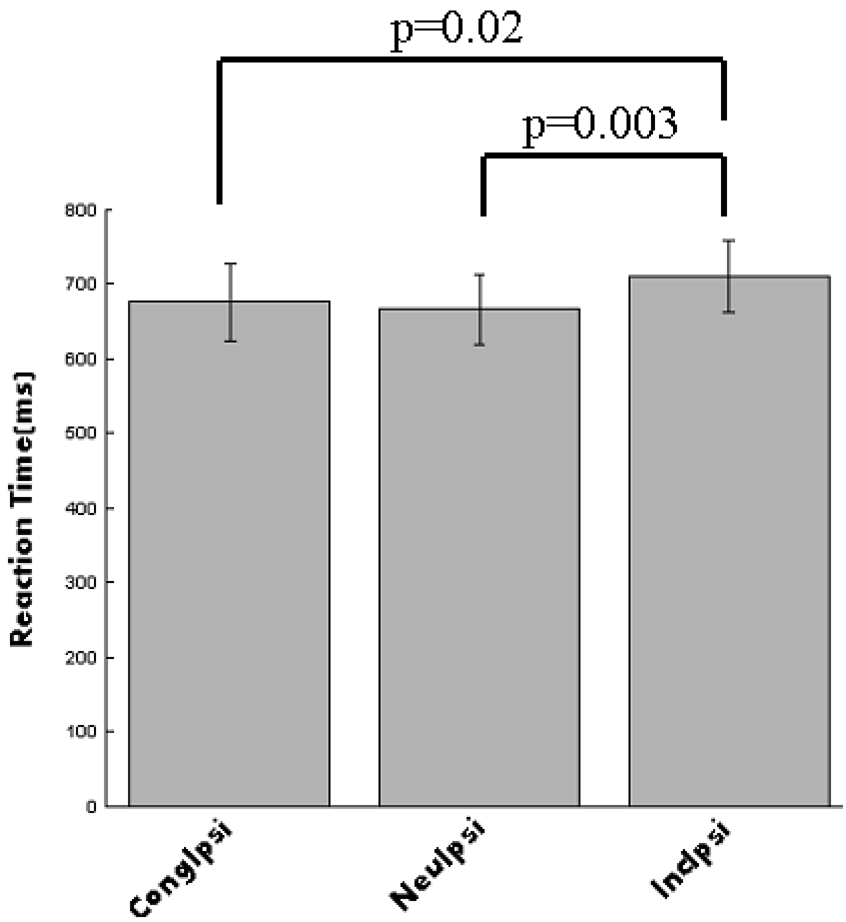

Figure 2. Behavioral Results: Mean RTs (±s.e.m.) across conditions for incongruent ipsilateral , neutral ipsilateral and congruent ipsilateral condition.A paired t-test indicated that responses were reliably slower in the incongruent ipsilateral condition than the neutral ipsilateral condition (t(13) = -3.5931, p=0.003). The congruent ipsilateral condition were responded to more quickly than incongruent ipsilateral condition (t(13) = -2.65, p=0.02). Note: CongIpsi-congruent= ipsilateral;NeuIpsi-neutral= ipsilateral;IncIpsi- incongruent= ipsilateral.

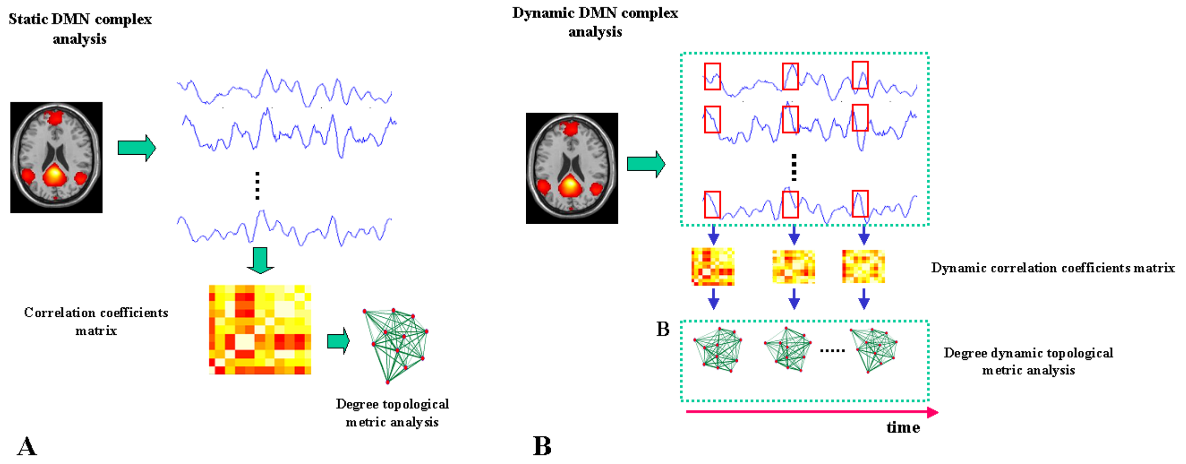

Figure 3. Analysis schematic. (A) Static DMN complex analysis .(B) Dynamic DMN complex analysis.

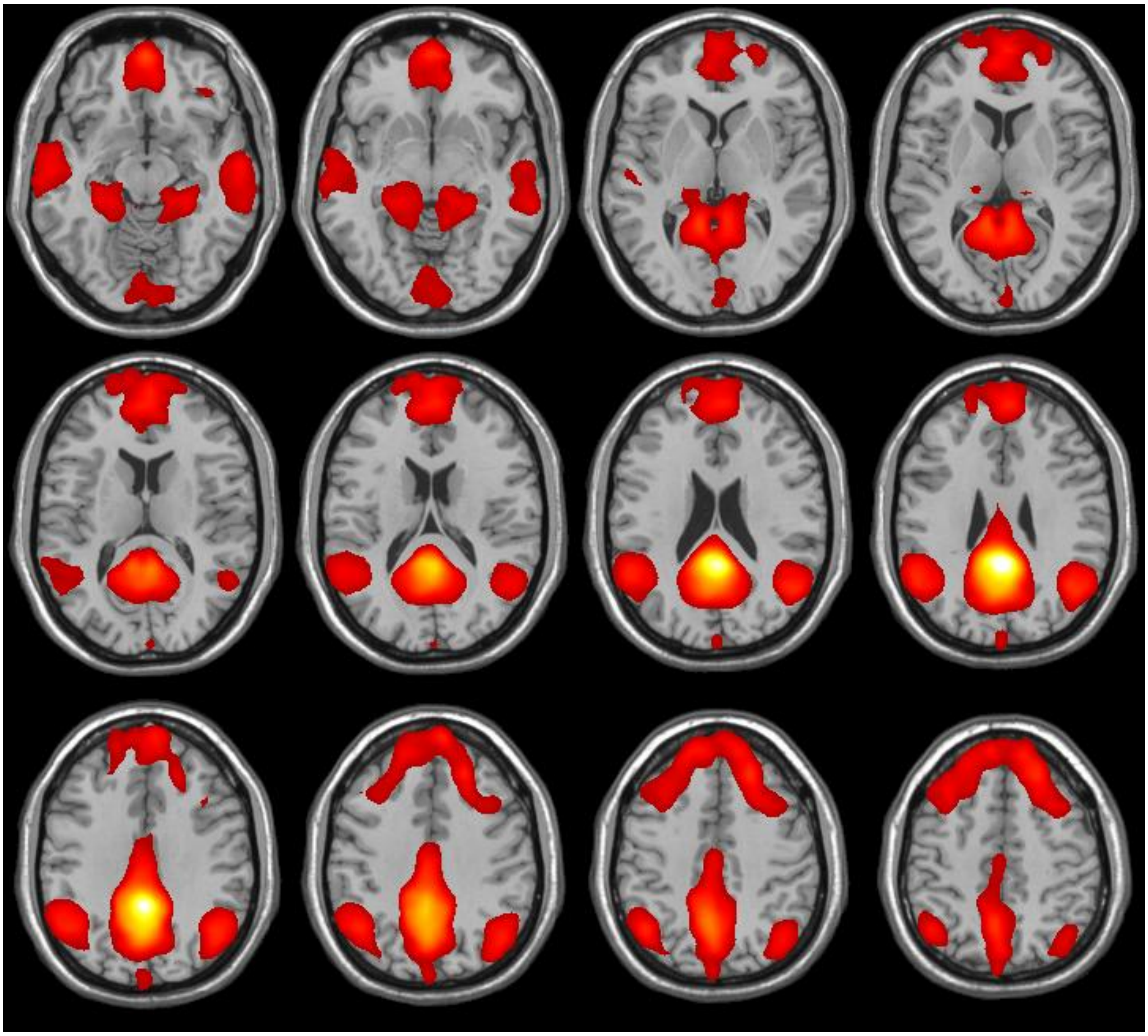

Figure 4. Group functional connectivity mapping of the posterior cingulate cortex during rest (cluster-level FWE-corrected p<0.05)

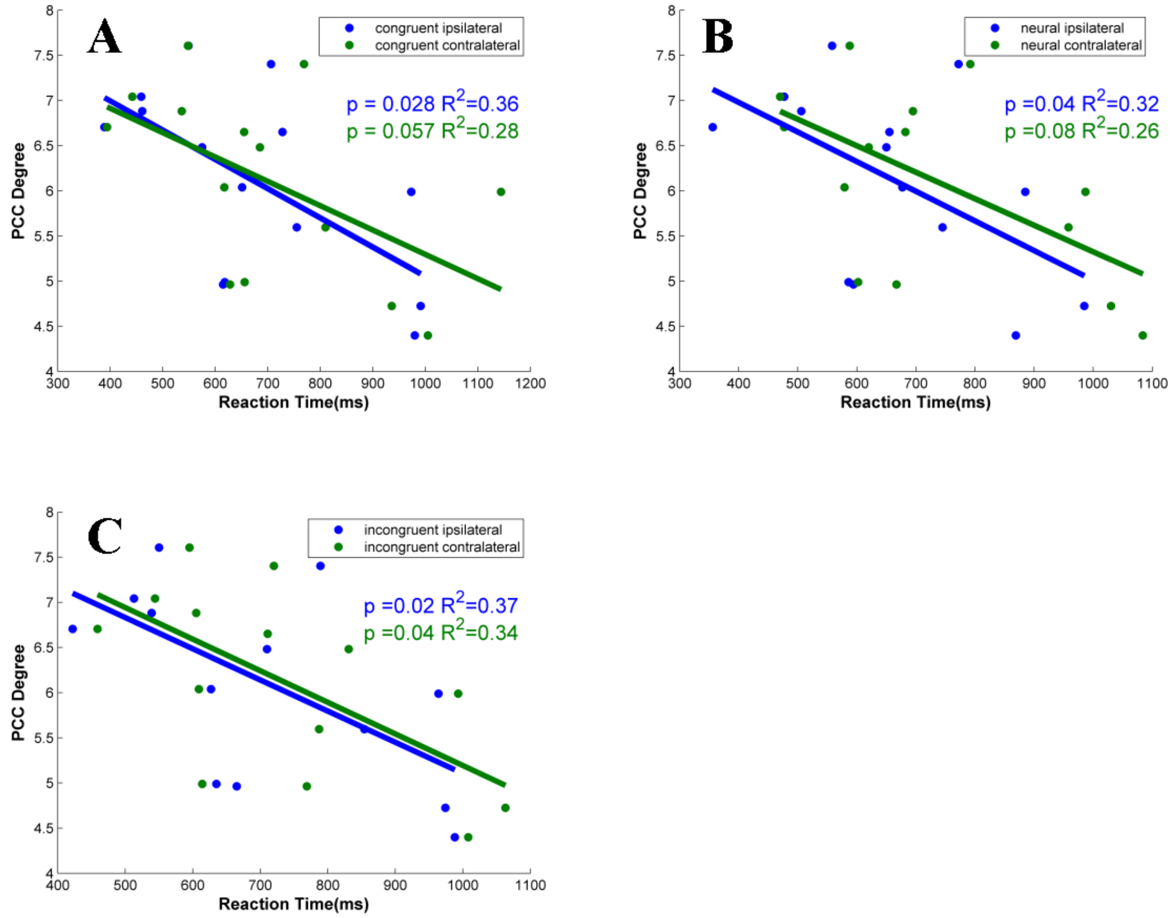

Figure 5. Relationship between PCC nodal topological metric and behavioral performance during attention task. Scatterplots of the association between task reaction time and PCC mean degree values. (A) shows the association between RT and PCC mean degree values for congruent ipsilateral (p=0.028,R^2 = 0.36) and congruent contralateral (p=0.057, R^2= 0.28); (B) shows the association between RT and PCC mean degree values for neutral ipsilateral (p=0.08, R^2= 0.26) and neutral contralateral (p= 0.04, R^2= 0.32). (C) shows the association between RT and PCC mean degree values for incongruent ipsilateral (p=0.04, R^2= 0.34) and incongruent contralateral (p= 0.02, R^2= 0.37).

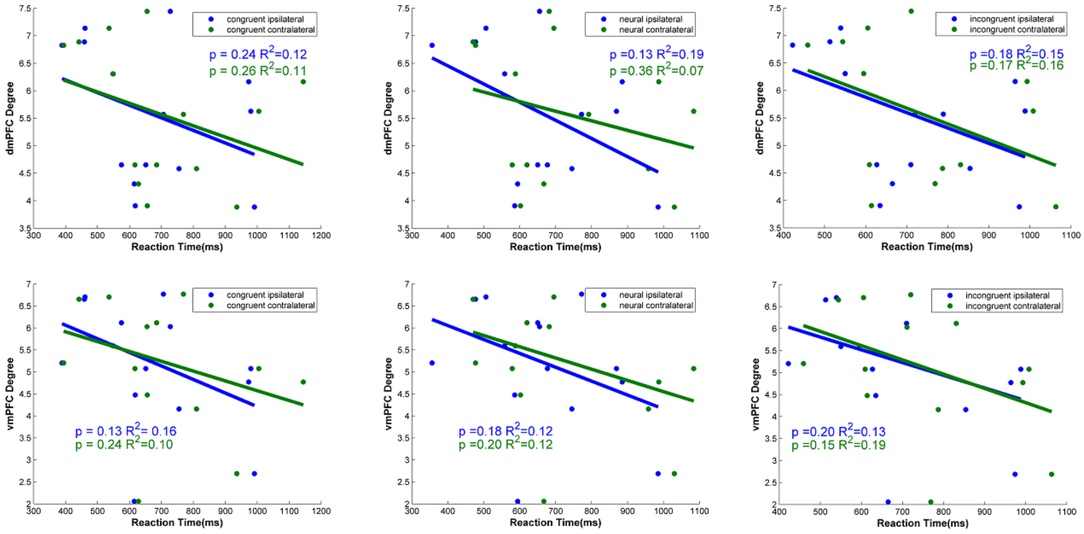

Figure 6. Relationship between brain–network metrics and behavioral performance. Scatterplots of the association between reaction time and dmPFC and vnPFC mean degree values. No significant correlation between them was observed (p>0.05).

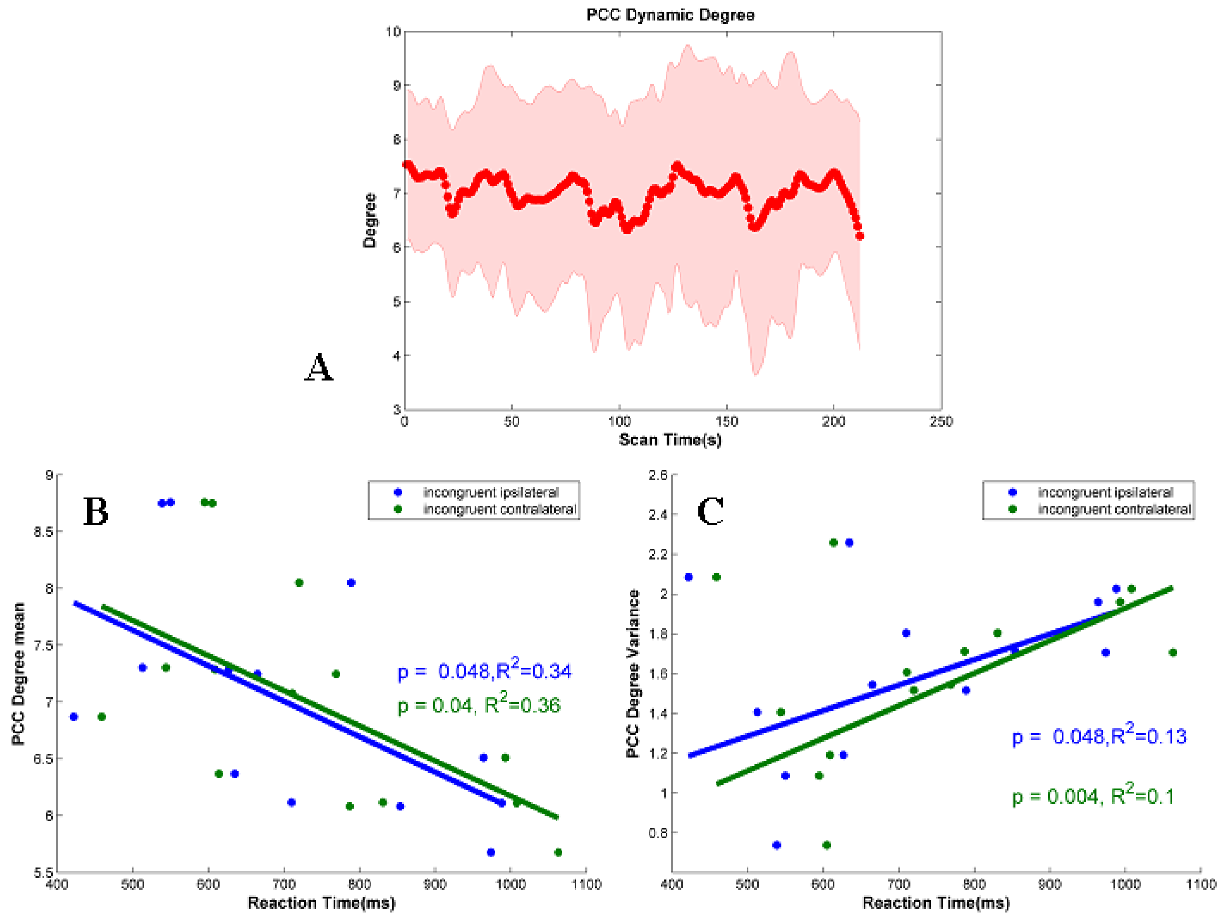

Figure 7. The relationship between dynamic resting-state DMN PCC degree and task performance based on 1 min sliding window analysis. (A) The mean dynamic time-evolving PCC degree topological properties within 14 subjects across the whole resting state period. (B) The association between RT and PCC dynamic degree values for incongruent ipsilateral (p=0.048, R^2= 0.34) and incongruent contralateral (p= 0.04, R^2=0.36). (C) The association between RT and variance of PCC dynamic degree for incongruent ipsilateral (p=0.048, R^2= 0.13) and incongruent contralateral (p= 0.004, R^2= 0.1). Shaded regions indicate standard error.

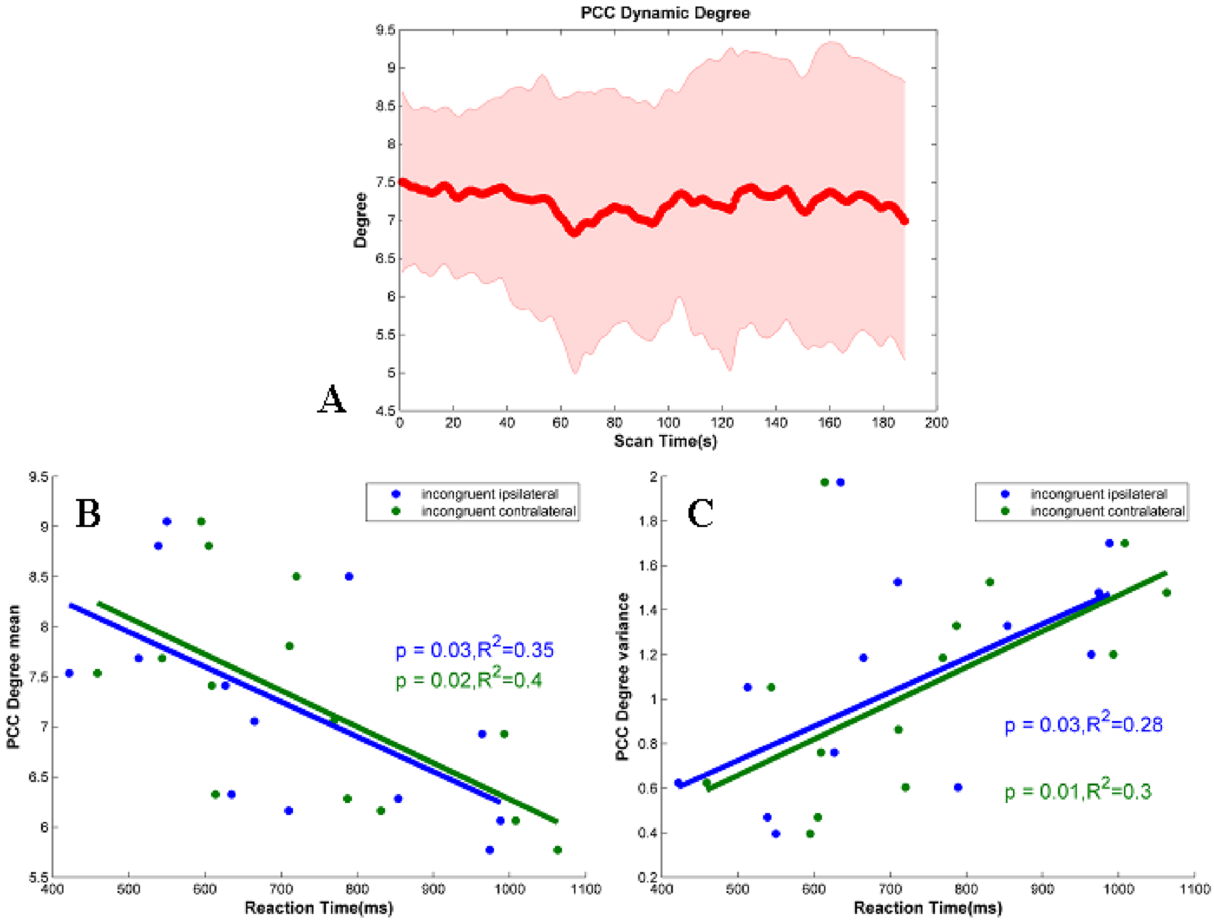

Figure 8. The relationship between dynamic resting-state DMN PCC degree and task performance based on 2 min sliding window analysis. (A) The mean dynamic time-evolving PCC degree topological properties within 14 subjects across the whole resting state period. (B) The association between RT and PCC dynamic degree values for incongruent ipsilateral (p=0.03, R^2= 0.35) and incongruent contralateral (p= 0.02, R^2=0.4). (C) The association between RT and variance of PCC dynamic degree for incongruent ipsilateral (p=0.03, R^2= 0.28) and incongruent contralateral (p= 0.01, R^2= 0.3). Shaded regions indicate standard error.